

THEORETICAL AND MATHEMATICAL
PHYSICS

Nonequilibrium Mechanisms of Weak Electrolyte Electrification under the Action of Constant Voltage

Yu. K. Stishkov* and V. A. Chirkov

St. Petersburg State University, Universitetskaya nab. 7-9, St. Petersburg, 199034 Russia

*e-mail: y.stishkov@spbu.ru

Received April 27, 2015

Abstract—The formation of space charge in weak electrolytes, specifically in liquid dielectrics, has been considered. An analytical solution is given to a simplified set of Nernst–Planck equations that describe the formation of nonequilibrium recombination layers in weak electrolytes. This approximate analytical solution is compared with computer simulation data for a complete set of Poisson–Nernst–Planck equations. It has been shown that the current passage in weak electrolytes can be described by a single dimensionless parameter that equals the length of a near-electrode recombination layer divided by the width of the interelectrode gap. The formation mechanism and the structure of charged nonequilibrium near-electrode layers in the nonstationary regime have been analyzed for different injection-to-conduction current ratios. It has been found that almost all charge structures encountered in weak dielectrics can be accounted for by the nonequilibrium dissociation–recombination mechanism of space charge formation.

DOI: 10.1134/S1063784216070276

INTRODUCTION

The space charge and its associated hydrodynamic processes are a basic feature of the behavior of weak dielectrics in a high electric field. The electrification of liquid dielectrics has been the subject of much research. In [1, 2], all charge structures experimentally found in liquid dielectrics were analyzed and described in terms of the electrolytic conduction mechanism.

In a number of earlier works [3, 4], simplified models of space charge formation in liquids with ionic conductivity were considered in the approximation of a strong electrolyte. However, liquid dielectrics are weak electrolytes in which the dissociation of impurity molecules is negligible, i.e., is much smaller than unity. For example, when iodine dissolves in transformer oil, the degree of dissociation of iodine does not exceed 10^{-6} [5, 6]. To describe the current passage in these liquids, a complete set of equations must contain functions that describe the dissociation and recombination of impurity molecules or, more properly, ionic pairs. In this work, we suggest a simple model that allows most charge structures that have been discovered to date to be considered from a single viewpoint based on the Nernst–Planck equations for weak electrolytes. Previously, the mechanism considered here was discussed in [7, 8].

It is known [5] that a high voltage accelerates the mechanism of injection nucleation on the surface of an electrolyte. Impurity molecules activate the injec-

tion; for example, an iodine molecule that offers increased electron–acceptor properties favors injection from the cathode.

Thus, three or perhaps four types of ions exist in a liquid dielectric subjected to a high voltage, i.e., two types of ions form through the self-dissociation of impurity molecules, $C = A^+ + B^-$ and one or two types of ions forming in near-electrode reactions (i) when an electron passes from the electrode surface to an impurity molecule $C + e = C^-$ that has increased electron–acceptor properties or (ii) when a molecule with increased electron–acceptor properties donates an electron $C - e = C^+$. These reactions proceed much more readily than dissociation reactions because of the presence of impurities that have a high electron affinity. Therefore, in the conductivity range below 10^{-10} S/m, injection dominates in charge generation.

Consider the simple problem of current passage in a liquid with low intrinsic conductivity at low and high voltages using the Poisson–Nernst–Planck equations

$$\operatorname{div}(\mathbf{E}) = \rho / \epsilon \epsilon_0, \quad (1)$$

$$\mathbf{E} = -\nabla \varphi, \quad (2)$$

$$\partial n_i / \partial t + \operatorname{div}(\mathbf{j}_i) = W - \alpha_r n_i n_{j \neq i}, \quad (3)$$

$$\mathbf{j}_i = n_i (Z_i b_i) \mathbf{E} - D_i \nabla n_i, \quad (4)$$

$$\rho = \sum_i Z_i e n_i. \quad (5)$$

Here, \mathbf{E} is the electric field strength, ρ is the space charge volume density, φ is the electrical potential, n is the concentration of ions, \mathbf{j} is the current density, \mathcal{W} is the dissociation rate, ε is the relative permittivity of the liquid, b is the ion mobility, D is the ion diffusion coefficient, α_r is the recombination coefficient, Z_i is the valence of ions, ε_0 is the dielectric constant, e is the unit electrical charge, and t is the time. Subscript i stands for the type of ion.

1. ANALYSIS OF THE NERNST–PLANCK EQUATIONS

Let us consider the 1D problem and make the following assumptions. There are only two types of ions, both types of ions are univalent, the diffusion coefficients and the absolute values of the mobilities of the ions are the same ($D_+ = D_- \equiv D$ and $b_+ = b_- \equiv b$, where the “+” and “-” signs indicate the type of ion), the liquid is isothermal, the dissociation rate does not depend on the electric field strength, and the degree of dissociation is small. All dimensional quantities were made dimensionless by dividing by their characteristic values as follows: the interelectrode gap, the electrode voltage, and the equilibrium ion concentration ($n_0 = \sigma_0/2eb$, where σ_0 is the low-voltage conductivity of the liquid). As the characteristic time, we took the time ions take to migrate through the interelectrode gap as follows: $\tau = L^2/bV_0$, where L is the interelectrode gap and V_0 is the voltage. Migration current density $j_0 = n_0bV_0/L$ was taken for the unit current density. The following boundary conditions were used: $x \in [0, 1]$, $\varphi(0) = 1$, $\varphi(1) = 0$, $j_+(0) = k_+$, $j_-(1) = k_-$, where k_{\pm} is the dimensionless density of the injection current at the boundary of the interelectrode gap ($k_{\pm} = j_{inj, \pm}/j_0$).

With regard to the above simplifications, the set of equations (1)–(5) can be written in the dimensionless form

$$d^2\varphi/dx^2 = -(n_+ - n_-)P_0/2, \quad (6)$$

$$\partial n_{\pm}/\partial t + \partial j_{\pm}/\partial x = P_0(1 - n_+n_-), \quad (7)$$

$$j_{\pm} = \mp n_{\pm}d\varphi/dx - P_D\partial n_{\pm}/\partial x, \quad (8)$$

where x is the dimensionless coordinate and

$$P_0 = \sigma_0L^2/bV_0\varepsilon\varepsilon_0, \quad (9)$$

$$P_D = D/bV_0 \quad (10)$$

are dimensionless parameters.

Set of equations (6)–(8) can be solved analytically under the following assumptions. First, the diffusion current is disregarded because of its smallness and the space charge is assumed to influence the electric field distribution insignificantly. Second, it is assumed that the size of the charged near-electrode layer is much smaller than the interelectrode gap (in essence, we consider a semi-infinite space). Third, a solution will only be sought for the stationary case. Finally, we

assume that injection from the electrodes is absent, i.e., $k_{\pm} = 0$. However, the latter assumption is not necessary; an analytical solution can be obtained at $k_{\pm} \in [0, 1]$.

As a result, the simplified set of equations can be represented as

$$dn_+/dx = P_0(1 - n_+n_-), \quad (11)$$

$$-dn_-/dx = P_0(1 - n_+n_-). \quad (12)$$

If $n_+ + n_- = 2n_0$, this set of equations has a simple solution (for the concentration of positive and negative ions), i.e.,

$$n_+ = 1 - 1/(1 + xP_0). \quad (13)$$

It follows from formula (13) that the ion concentration is nonuniformly distributed near the electrode and parameter P_0 determines the thickness of a layer with a lower ion concentration; the smaller P_0 , the thinner the layer, and vice versa. Since only the dissociation–recombination mechanism of ion generation is taken into account in initial equations (11) and (12), we can suppose that the reason for the appearance of the ion is the disturbance of dissociation–recombination equilibrium after the voltage is switched on, i.e., ion migration. Parameter P_0 in the solution is the ratio of the interelectrode gap length to the size of the near-electrode nonequilibrium layer. If P_0 is large, the size of the layer is much smaller than the gap length.

It follows from solution (13) that nonequilibrium near-electrode layers with a lower ion concentration arise in the interelectrode gap. Dimensionless parameter P_0 is the ratio of two characteristic lines, i.e., the migration time ($\tau_1 = L^2/bV_0$) and the time of Maxwellian relaxation ($\tau_2 = \varepsilon\varepsilon_0/\sigma_0$). The same parameter P_0 characterizes the influence of the space charge on an external electric field. Let us analyze the dimensionless parameters in the given set of equations. According to (7), parameter P_0 characterizes the role of recombination–dissociation processes in the volume. If P_0 is large, dissociation in the volume plays a great role, as a result of which the equilibrium concentrations of ions are rapidly established in most of the volume. That is, the disturbance of the concentration due to the boundary conditions (for example, due to the absence of injection from the walls) is rapidly compensated for and does not penetrate into the interelectrode gap. This means that the nonequilibrium layers are thin compared with the gap length.

Parameter P_D is the ratio between the diffusion and migration components of the current density. Its role is significant in strong electrolytes and at low voltages. In the case of weak electrolytes, which liquid dielectrics are, and at high voltages, as a rule, this parameter is very small.

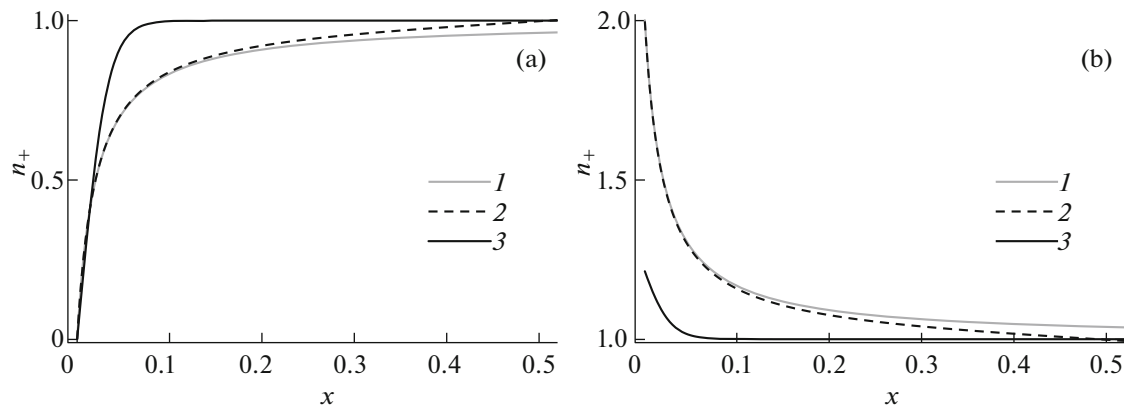


Fig. 1. Dimensionless concentration distributions for (a) positive and (b) negative ions constructed based on the (1) analytical solution and (2) simplified and (3) complete statements of the problem. $P_0 = 50$.

2. STATIONARY SOLUTION

Let us consider the results of the numerical solution of Eqs. (6)–(8) that were obtained with and without the above simplifications. Calculations were carried out using the COMSOL Multiphysics program package based on the finite element method. To avoid poor numerical convergence of the solution in the nonstationary regime and obtain the most exact solution possible, the nonstationary 1D problem was transformed into a 2D problem, where the y coordinate is time. This approach is used to numerically solve the problem of shock-front propagation.

The stationary distributions of the dimensionless concentrations of positive and negative ions in the interelectrode gap are shown in Fig. 1, which depicts three plots, including the analytical solution and numerical solutions obtained in the complete and simplified (i.e., without regard to the influence of the space charge on the electric field strength and under the assumption of reduced diffusion) statements of the problem. The plots show only the right-hand part of the gap. It can be seen that the analytical solution and the numerical solution in the simplified statement nearly coincide but differ somewhat from the exact solution. In all cases, recombination layers arise but taking into account the space charge somewhat changes the structure of the layers. Namely, the concentration of positive ions falls more steeply and that of negative ions becomes much lower. The main reason for the quantitative discrepancy is that the change in the electric field distribution under the action of the space charge concentrated in near-electrode layers was ignored. Nevertheless, the characteristic length of the layer is correctly described in all the cases.

Some comments regarding the obtained solution. An applied voltage generates a directed ion flux in the volume of the film, since the film is conductive. However, the flux and concentration of ions of the same sort vanish at the electrode boundary because of the presence of a wall on which surface nucleation is

absent. As a result, the concentration of like ions in the near-electrode region becomes insufficient. Inside this region, which is distinctly seen in Fig. 1a, the ion concentration grows from zero to an equilibrium value by means of dissociation nucleation. The characteristic size of the layer depends on the ratio between the dissociation rate and migration current or, as follows from the analytical solution, on dimensionless parameter P_0 .

The change in the negative ion concentration (Fig. 1b), which arises when the influence of the space charge on the electric field is taken into account, causes a decrease in the recombination rate inside the near-electrode layer. This in turn enhances nucleation in the volume. This is exactly why the near-electrode layer gets slightly thinner (Fig. 1a) in the numerical solution compared with the approximate solution.

3. NUMERICAL SOLUTION OF THE COMPLETE SET OF EQUATIONS

Consider the solution of the problem in the complete statement, i.e., without the assumption that the space charge weakly influences the electric field. Except for dimensionless parameter P_0 , the simulation results depend on the boundary conditions, namely, on dimensionless injection current k_{\pm} on the electrodes. Consider first the case when injection is absent: $k_{\pm} = 0$. Below, linear plots for different values of dimensionless parameter P_0 are presented.

3.1. Dissociation without Injection: $P_0 = 0.05$

Since injection is absent and the ion generation rate (dissociation rate) is the same throughout the volume, the coion deficiency front moves from either electrode (Fig. 2a). This front produces a region with a lower concentration of coions (i.e., a region with oppositely charged ions) at either electrode (Fig. 2b). Because of heterocharge layers that form at the elec-

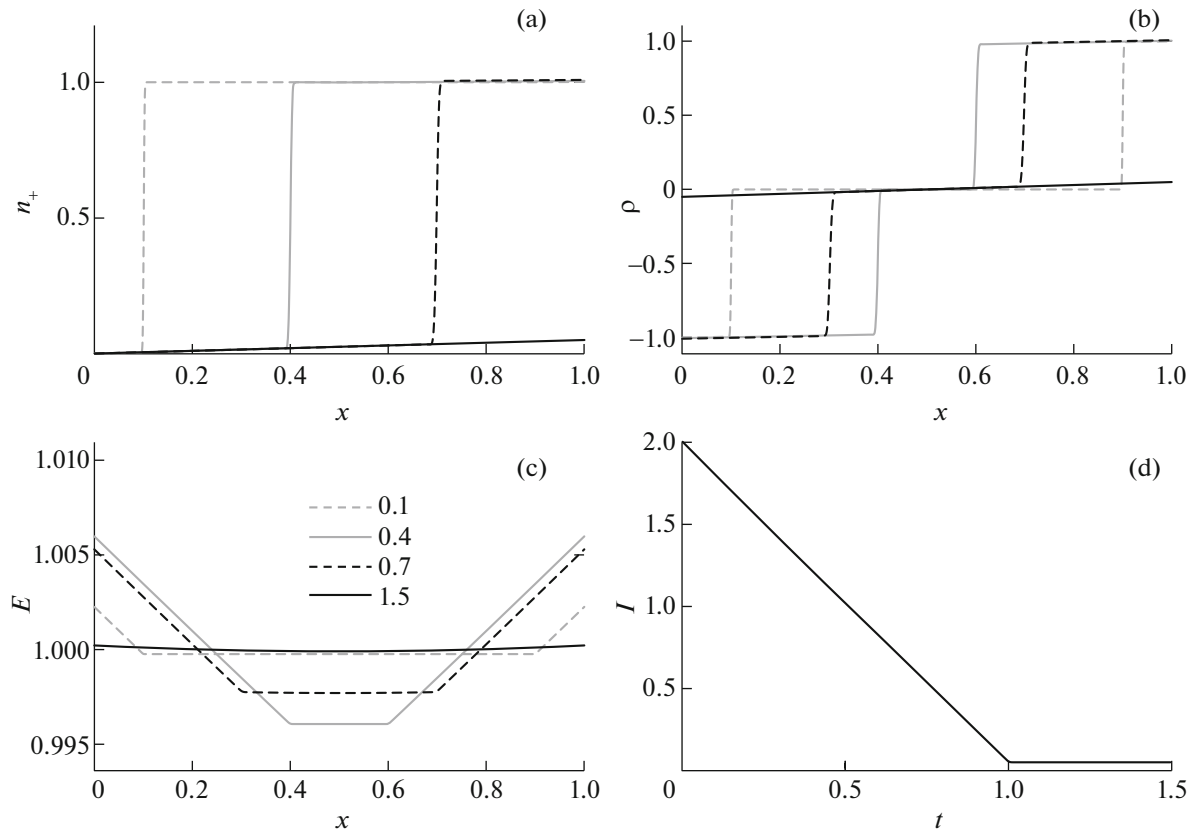


Fig. 2. Distributions of the dimensionless (a) concentration, (b) space charge density, (c) electric field strength, and (d) total current at several instants of time for $P_0 = 0.05$ (without injection). Hereinafter, the time scale for panels (a–c) is plotted in panel (c).

trodes, the electric field strength near the electrodes rises and drops at the center of the interelectrode gap (Fig. 2c). The fronts meet at the center of the gap and pass through each other, compensating for the resulting charged layers. This compensation is incomplete because of a persisting dissociation in the volume. However, as follows from the analysis of dimensionless parameter P_0 , the characteristic time of volume nucleation in the given case is 20 times longer than the time it takes for the ion front to cross the interelectrode gap. Therefore, dissociation may compensate for only a minor part of charge loss at the electrodes. As a result, the effective conductivity of the cell drastically decreases, as is seen, in particular, in the time–current characteristic (TCC) depicted in Fig. 2d; the current drops by more than an order of magnitude.

3.2. Dissociation without Injection: $P_0 = 0.5$

When dimensionless parameter P_0 increases by ten times, first the significance of dissociation–recombination processes in the volume grows. This is reflected in the fact that, within the time the ion front crosses the interelectrode gap, new ions due to dissociation emerge in the volume (Fig. 3a). As the fronts move, the total concentration of ions of both signs grows

(Fig. 3a, an area near the electrode on the right). Heterocharge layers arise near the electrodes (Fig. 3b), and the space-charge-induced variation of the electric field distribution becomes tangible (Fig. 3c). In the TCC (Fig. 3d), the current drops, but this drop is less significant, unlike the previous case (the field changes by roughly four times).

3.3. Dissociation without Injection: $P_0 = 10$

When dimensionless parameter P_0 is greater than unity, the dissociation nucleation dominates over current transfer by migration, even at small distances compared with the interelectrode gap. Therefore, an equilibrium concentration is reached well before ions cross the gap. As a result, a clear-cut dissociation–recombination layer of like ions appears near either electrode (Fig. 4a). In addition, an area of excess heterocharge localizes within this layer (Fig. 4b). In the rest of the interelectrode gap, the liquid is electroneutral and the concentration distribution is equilibrium. With an increase in the dimensional parameter, the electric field in the near-electrode layers locally grows (Fig. 4c), but the enhanced field region shrinks, since the heterolayers become thinner. The current relaxation time also diminished considerably (Fig. 4d) and

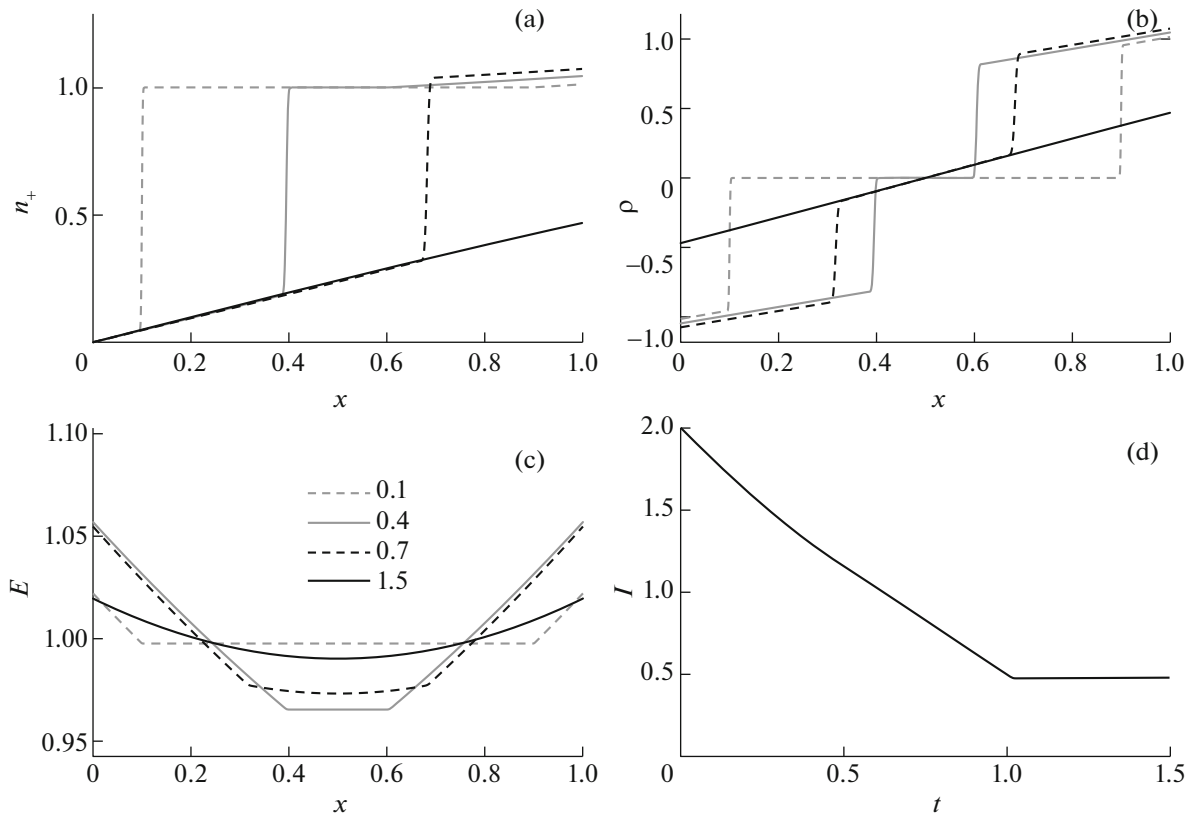


Fig. 3. Distributions of the dimensionless (a) concentration, (b) space charge density, (c) electric field strength, and (d) total current at several instants of time for $P_0 = 0.5$ (without injection).

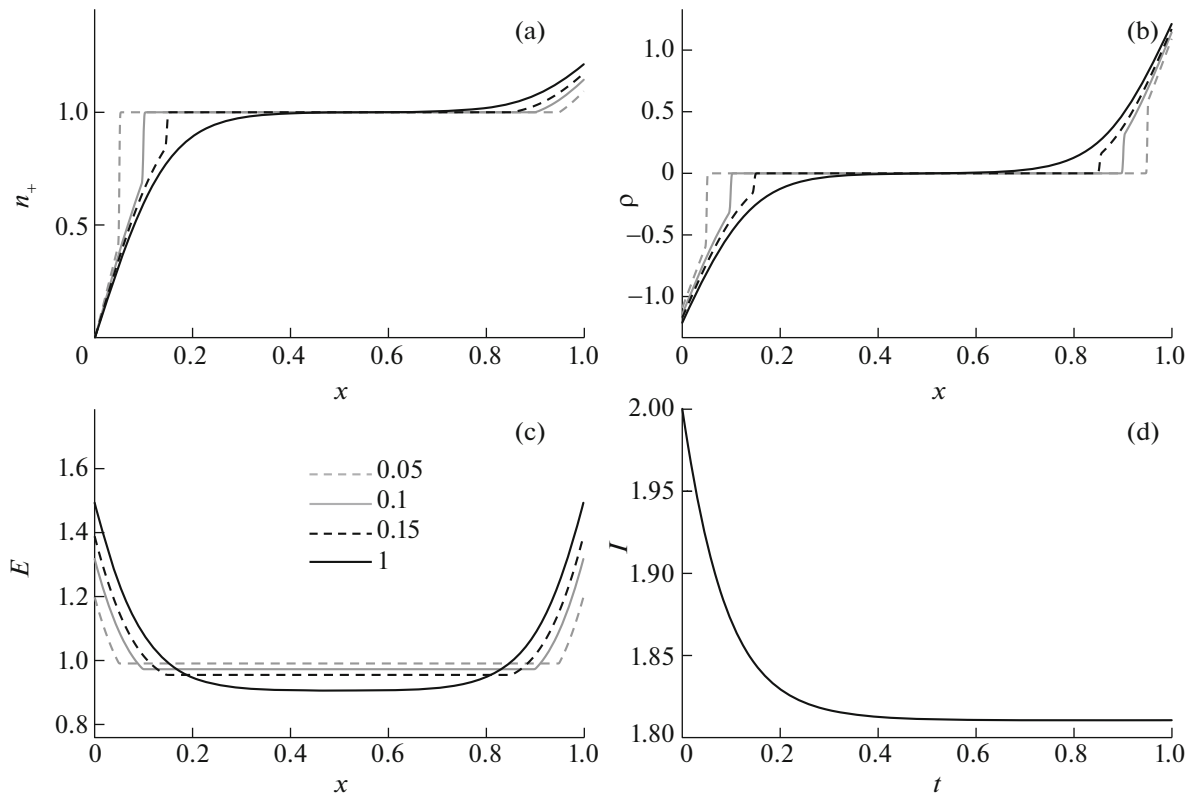


Fig. 4. Distributions of the dimensionless (a) concentration, (b) space charge density, (c) electric field strength, and (d) total current at several instants of time for $P_0 = 10$ (without injection).

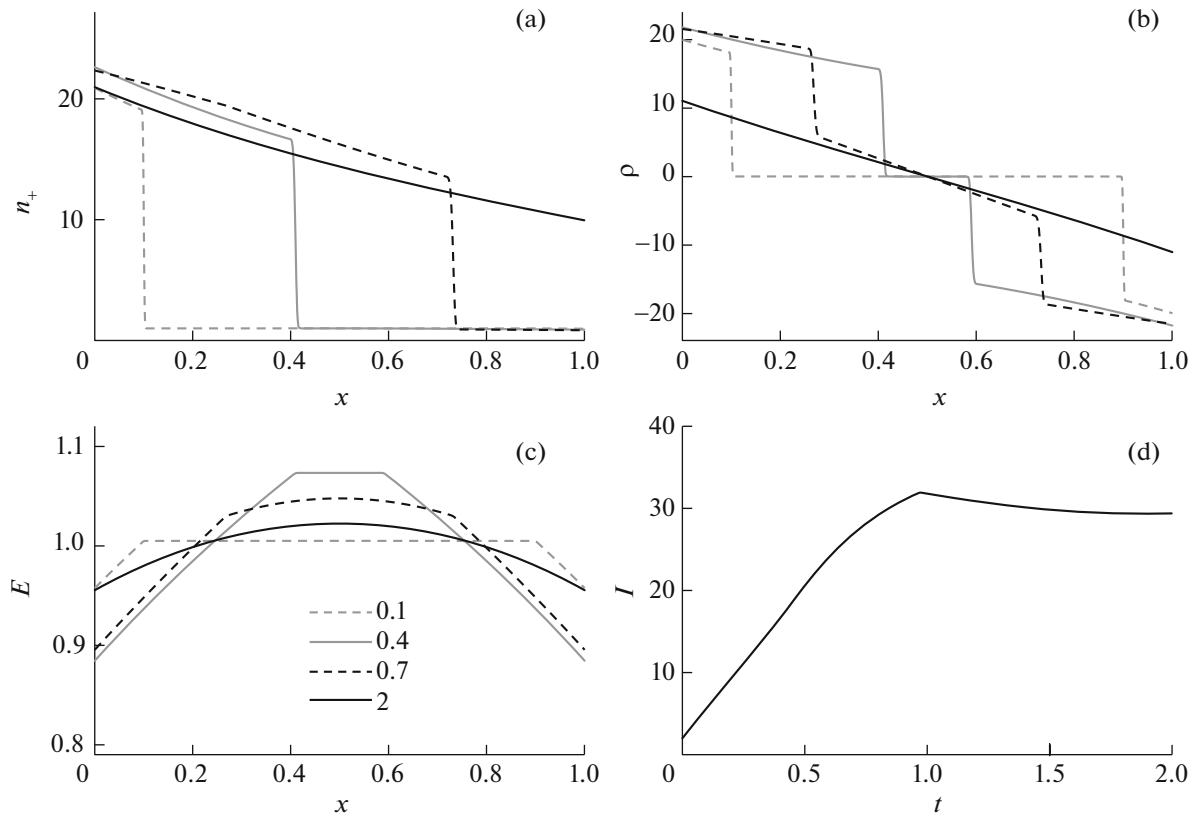


Fig. 5. Distributions of the dimensionless (a) concentration, (b) space charge density, (c) electric field strength, and (d) total current at several instants of time for $P_0 = 0.05$ and $k_{\pm} = 20$.

the drop of the cell's effective conductivity decreased to 20%. Here, the time it takes for ions to pass through the near-electrode layer, rather than through the entire gap, is the characteristic time to steady-state distribution. Thus, the simulation data show that the distributions of the desired quantities are similar to each other and depend on the near-electrode layer P_0 .

3.4. Dissociation with Bipolar Injection: $P_0 = 0.05, k_{\pm} = 20$

Consider the simulation data for the case of intense bipolar injection from both electrodes when the concentration of injected ions exceeds the equilibrium value by 20-fold, i.e., $k_{\pm} = 20$ and $P_0 = 0.05$.

In real liquids subjected to a high voltage, ions are injected into a liquid that has an intrinsic low-voltage conductivity. It was found from I - V characteristics that the low-voltage conductivity portion changes to high-voltage conductivity at a certain threshold voltage. This threshold voltage marks the onset of injection. Let us consider a model of injection into a liquid with a constant low-voltage conductivity. In other words, consider the case of bipolar injection into a liquid having an intrinsic low-voltage conductivity.

Let us start with the situation when dissociation-recombination processes play a minor role. This situation most closely resembles injection into a nonconducting liquid. Consider the case when the injection current density greatly exceeds the conductivity current density ($k_{\pm} = 20$). As follows from the plot in Fig. 5a, the fronts of elevated ion concentration propagate from the electrodes in the liquid but the amplitudes of the fronts drop (roughly twofold) because of recombination with counter ions, which arise in the volume by means of dissociation on the surface and are injected from the opposite electrode. The excess of coions in the near-electrode layers generates a space charge of the same sign as the electrode (Fig. 5b). This in turn reduces the electric field strength near both electrodes and raises it at the center of the interelectrode gap (Fig. 5c). Since the total concentration of ions in the volume of the liquid rises during the transient process, the current in the TCC grows (Fig. 5d). However, after the fronts of oppositely charged ions meet, the recombination rate in the volume rises and the current rise somewhat slows down. Then, after the fronts reach the counter electrodes, the current slightly decreases. This is an example of the case when recombination in the volume noticeably influences both the local distributions of desired quantities and the integral characteristics of the cell, causing the total current to decline.

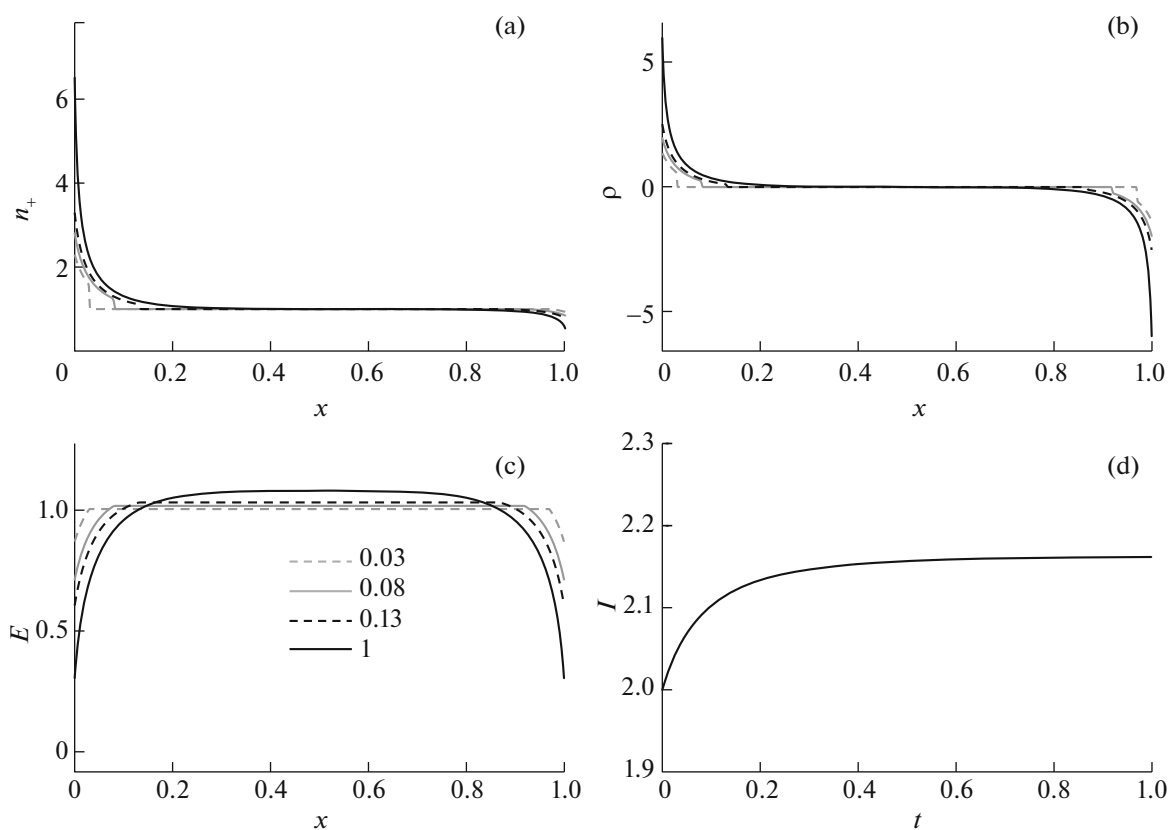


Fig. 6. Distributions of the dimensionless (a) concentration, (b) space charge density, (c) electric field strength, and (d) total current at several instants of time for $P_0 = 10$ and $k_{\pm} = 2$.

3.5. Dissociation with Bipolar Injection:

$$P_0 = 10, k_{\pm} = 2$$

Consider now the case when dissociation–recombination processes in the volume are significant and injection nucleation on the electrodes is set. Then, the amplitude of the higher ion concentration front (Fig. 6a) rapidly decays near the injecting electrodes and the homocharge fronts do not penetrate into the interelectrode gap. This is because recombination processes dominate under the given conditions. Importantly, this charge decay takes place in the one-dimensional system, where the ion concentration cannot decrease because of the ion spread in the transverse direction. As a result, two injection–recombination near-electrode layers of homocharge appear in the liquid (Fig. 6b), the size of which is comparable to that of dissociation–recombination near-electrode layers of heterocharge, which was estimated above for the same value of P_0 but without injection. The electric field strength near either electrode decreases under the action of the homocharge, but this field disturbance area narrows (Fig. 6c). The TCC shows a slight current rise (by less than 10%), while the injection current exceeds the conduction current twofold (Fig. 6d).

CONCLUSIONS

When the current passes through weak electrolytes, the liquid dielectrics of which are nonequilibrium, dissociation–recombination layers arise. In the absence of injection, layers with a lower effective conductivity form at the electrodes. This is reflected in the fall of the total current in the cell. Accordingly, when measuring the low-voltage conductivity of liquid dielectrics, one should provide conditions such that $P_0 \gg 1$ to obtain correct results.

The structure of the layers depends considerably on dimensionless current density k_{\pm} . At $k_{\pm} < 1$, injected ions recombine with conduction ions in the near-electrode layers and do not penetrate into the volume of the liquid. At $k_{\pm} = 1$, injected ions are absent. At $k_{\pm} > 1$, injected ions only effectively penetrate into the volume if dimensional parameter P_0 is small; otherwise ($P_0 > 1$), injected ions rapidly recombine, which produces an injection–recombination layer with characteristic penetration length $1/P_0$.

Even if injected ions penetrate into the liquid through the counterflow of conduction ions, they influence the total current that passes through the cell insignificantly at $P_0 \gg 1$. Therefore, analyzing experimental data on the I – V characteristic of a cell with a

liquid electrolyte, one may draw improper conclusions regarding the role of the injection current. For example, even a small deviation of the integral current–voltage dependence from a linear law may indicate that the injection current density greatly exceeds the conduction current density (especially if the problem has no 1D symmetry).

The nonequilibrium dissociation–recombination mechanism of space charge formation can explain the nearly entire spectrum of charge structures discovered in liquid dielectrics, as well as the threshold nature of electrohydrodynamic effects. Note that this mechanism works even in slightly nonuniform fields, which is also typical of electrohydrodynamic flows [2].

ACKNOWLEDGMENTS

This work was supported by St. Petersburg State University (grant no. 1.0.65.2010). Calculations were performed at St. Petersburg Computing Center (<http://cc.spbu.ru>).

REFERENCES

1. F. P. Grosu, M. K. Bologa, V. V. Bloschitsyn, Yu. K. Stishkov, and I. V. Kozhevnikov, *Elektron. Obrab. Mater.* **43** (5), 16 (2007).
2. Yu. K. Stishkov and A. A. Ostapenko, *Electrohydrodynamic Flows in Fluid Dielectrics* (Izd. Leningr. Univ., Leningrad, 1989).
3. A. A. Vartanyan, V. V. Gogosov, V. A. Polyansky, and G. A. Shaposhnikova, *J. Electrostat.* **23**, 431 (1989).
4. V. A. Polyansky and I. L. Pankratieva, *J. Colloid Interface Sci.* **230**, 306 (2000).
5. Yu. K. Stishkov, *Dokl. Akad. Nauk SSSR* **288** (4), 861 (1986).
6. Yu. K. Stishkov and Yu. M. Rychkov, *Elektron. Obrab. Mater.*, No. 6, 44 (1981).
7. N. M. Semenikhin and E. K. Zholkovskii, *Elektrokhimiya* **18**, 691 (1982).
8. A. I. Zhakin, *Phys. Usp.* **49**, 275 (2006).

Translated by V. Isaakyan